Cukurova Medical Journal
ÇUKUROVA ÜNİVERSİTESİ TIP FAKÜLTESİ

Cukurova Med J 2024;49(1):89-96
DOI: 10.17826/cumj.1393084

RESEARCH

Machine learning-based analysis of MRI radiomics in the discrimination of classical and non-classical polycystic over syndrome

Klasik ve klasik olmayan polikistik over sendromunun ayrımında MRG radyomik özelliklerin makine öğrenimine dayalı analizi

Günay Rona[1], Neriman Fıstıkçıoğlu[1], Ahmet Tekin Serel[2], Meral Arifoğlu[1], Hanife Gülden Düzkalır[1], Şehnaz Evrimler[3], Serhat Özçelik[1], Kadriye Aydın[1]

[1]University of Health Sciences, İstanbul, Turkey
[2]Suleyman Demirel University, Isparta, Turkey
[3]Ankara Etlik City Hospital, Ankara, Turkey

Abstract

Purpose: The aim of this study is to investigate the value of radiomics analysis on T2-weighted Magnetic Resonance imaging (MRI) images in differentiating classical and non-classical polycystic ovary syndrome (PCOS).

Materials and Methods: A total of 202 ovaries from 101 PCOS patients (mean age of 23±4 years) who underwent pelvic MRI between 2014 and 2022, were included in the study. Of the patients, 53 (52.5%) were phenotype A, 12 (11.9%) were phenotype B, 25 were phenotype C (25.1%), and 11 were phenotype D (10.9%). 130 (64.4%) of the ovaries were classical PCOS, 72 (35.6%) were non-classical PCOS. The ovaries were manually segmented in all axial sections using the 3D Slicer program. A total of 851 features were extracted. Python 2.3, Pycaret library was used for machine learning (ML) analysis. Datasets were randomly divided into train (70 %, 141) and test (30 %, 61) datasets. The performances of ML algorithms were compared with AUC, accuracy, recall, precision and F1 scores.

Results: Accuracy and AUC values in the training set ranged from 57%-73% and 0.50-0.73, respectively. The two best ML algorithms were Random Forest (rf) (AUC:0.73, accuracy:73%) and Gradient Boosting Classifier (gbc) (AUC:0.71, accuracy:70%). AUC, accuracy, recall and precision values and F1 score of the blend model obtained from these two models were 0.70, 73 %, 56 %, 66%, 58%, respectively.

Conclusion: Radiomic features obtained from T2W MRI are successful in distinguishing between classical and non-classical PCOS.

Keywords:. Polycystic ovary syndrome, phenotypes, magnetic resonance imaging, machine learning, radiomics, texture analysis

Öz

Amaç: Bu çalışmanın amacı, klasik ve klasik olmayan polikistik over sendromunu (PKOS) ayırmada T2 ağırlıklı Manyetik Rezonans görüntüleme (MRG) görüntüleri üzerinde radyomik analizin değerini araştırmaktır.

Gereç ve Yöntem: Çalışmaya 2014-2022 yılları arasında pelvik MRG çekilen 101 PKOS hastasına ait (ortalama yaş 23±4) 202 over dahil edildi. Hastaların 53'ü (%52,5) fenotip A, 12'si (%11,9) fenotip B, 25'i fenotip C (%25,1) ve 11'i (%10,9) fenotip D idi. Overlerin 130'u (%64,4) klasik PKOS, 72'si (%35,6) klasik olmayan PKOS idi. Overler 3D Slicer programı kullanılarak tüm aksiyel kesitlerde manuel olarak segmente edildi. Toplam 851 özellik çıkarıldı. Makine öğrenimi (ML) analizi için Python 2.3, Pycaret Library programı kullanıldı. Veri kümeleri rastgele eğitim (%70, 141) ve test (%30, 61) veri kümelerine bölündü. ML algoritmalarının performansları AUC, doğruluk, hatırlama, kesinlik ve F1 puanlarıyla karşılaştırıldı.

Bulgular: Eğitim setindeki doğruluk ve AUC değerleri sırasıyla %57-%73 ve 0,50-0,73 arasındaydı. En iyi iki makine öğrenimi algoritması Random Forest (rf) (AUC:0,73, doğruluk: %73) ve Gradient Boosting Classifier (gbc) (AUC:0,71, doğruluk: %70) idi. Bu iki modelden elde edilen harman modelinin AUC, doğruluk, hatırlama ve kesinlik değerleri ile F1 puanı sırasıyla 0,70, %73, %56, %66, %58 olarak bulunmuştur.

Sonuç: T2A MR'dan elde edilen radyomik özellikler klasik ve klasik olmayan PKOS ayrımında faydalıdır.

Anahtar kelimeler: Polikistik over sendromu, fenotipler, manyetik rezonans görüntüleme, makine öğrenimi, radyomik, doku analizi

Address for Correspondence: Günay Rona, University of Health Sciences, Kartal Doktor Lütfi Kırdar Training and Research Hospital, Department of Radiology, İstanbul,Turkey E- mail: gunayrona@gmail.com
Received: 25.11.2023 Accepted: 07.02.2024

INTRODUCTION

Polycystic ovary syndrome (PCOS) is a heterogeneous disease characterized by ovarian dysfunction and hyperandrogenism. In addition to affecting the reproductive system, obesity is associated with insulin resistance, type 2 diabetes mellitus, dyslipidemia and metabolic syndrome [1].

The clinical presentation varies over a widely. Most patients exhibit irregular menstrual cycles, acne, hirsutism, obesity and insulin resistance. However, some patients only have dysfunctional ovaries with polycystic ovary morphology (PCOM)[1,2]. Due to this broad clinical spectrum confuses diagnosis, phenotypes of PCOS were established. In 2012, four phenotypes were defined by the NIH consensus panel: A, B, C, and D [3]. Identifying phenotypes is crucial as treatment approach varies[1].

Diagnosis involves menstrual irregularity, hyperandrogenism (clinical or biochemical) and the presence of PCOM on ultrasound (US)[4]. Transvaginal US reveals 12 or more follicles with a diameter of 2-9 mm and an ovarian volume of more than 10 cm^3 are indicative of PCOM[5-8]. MRI is a useful and reliable test in obese and young patients when transabdominal US is insufficient in and vaginal probes cannot be used[9-14]. T2W images on MRI can successfully depict the morphology and internal structure of the ovary in PCOS[12-14]. Increased ovarian volume, an abundance of immature follicles peripherally distributed are the diagnostic criteria for PCOS. It is suggested that MRI is more sensitive than US in determining ovarian volume and follicle number[9-12,15]. Some argue that with MRI, PCOS can be diagnosed earlier in obese patients, enabling earlier treatment and prevention of complications[11,12].

Radiomics is a technique that derives a comprehensive set of imaging features are derived from a specific region of interest[16]. Extracted features include volume, shape, surface, density and intensity, texture, spatial location, and relationships with adjacent tissues. First-order features provide information about pixel intensity, while second-order features describe the relationship between pixels and voxels[17].

The clinical presentation of PCOS is heterogeneous and varies according to phenotypes. Typical findings of PCOS are observed in Phenotypes A and B, considered classical PCOS. In phenotypes C and D, the findings are milder describing nonclassical PCOS. The value of radiological findings in distinguishing between classical and nonclassical PCOS is not clear. Our aim in this study is to investigate the performance of radiomic features obtained from T2-weighted (T2W) MR sequences in differentiating classical PCOS and non-classical PCOS using machine learning (ML) analysis.

MATERIALS AND METHODS

Ethics committee approval was obtained from our institution for this retrospective study (Kartal Doctor Lütfi Kırdar City Hospital, date: 29.05.2023, approve no: 202351425035). Informed consent was not obtained from the patients, as it was a retrospective study.

Study population

Female patients who were diagnosed with PCOS in the endocrinology department of Kartal Doctor Lütfi Kırdar City Hospital between January 2014 and June 2022, and who underwent pelvic MRI, were filtered from the hospital database. Pelvic MRI was performed for reasons other than PCOS diagnosis, such as pelvic pain and inflammatory bowel disease that could not be diagnosed with US. Patients who did not undergo pelvic MRI were excluded from the study.

The diagnosis of PCOS was made by endocrinologists with 10 and 7 years of experience in the field of PCOS. PCOS diagnosis was accepted as PCOS if at least two of the Rotterdam criteria (a) oligo or anovulation, b) clinical or biochemical hyperandrogenism, c) PCOM appearance on US) were met (12). High serum androgen levels (testosterone ≥ 60 ng/dl) and/or a high free androgen index (FAI) (≥49) were considered biochemical hyperandrogenism[18]. A modified Ferriman-Gallwey (FG) score of ≥7 was considered clinical hyperandrogenism[19]. Diseases causing hyperandrogenism and oligo-ovulation / anovulation such as non-classical congenital adrenal hyperplasia, hyperprolactinemia, thyroid dysfunction, Cushing's syndrome and androgen producing tumors, were excluded.

The phenotypes of the patients were determined according to the 2012 NIH consensus panel. Due to the number of patients, they were divided into two groups: phenotype A+B and phenotype C+D. Phenotype A+B was labeled as group 1(classical PCOS), and phenotype C+D as group 2 (non-classical PCOS). The ovaries of the patients in group 1 and group 2 were included in the study.

MRI acquisition

MRI examinations were performed with a 1.5 T MRI device (Philips Ingenia, Philips Healthcare, Best, The Netherlands) using a dedicated 32-channel phased array body coil. MRI examinations were conducted after 8 hours of fasting. Images were taken in the supine position while holding the breath. Non-fat-saturated turbo-spin-echo axial T2W (Field of View (FOV): 311x311 mm, Matrix: 224x206, Flip Angle (FA): 90 deg, Repetition Time (TR): 7181 ms, Echo Time (TE): 90 ms, Slice thickness: 6.00 mm, Slice gap: 5.00) and (FOV:288x288 mm, Matrix: 292x273, FA: 90 degrees, TR: 2558, TE: 90, 90 ms, Slice thickness: 5.00 mm, Slice gap: 5.00) images were obtained.

Feature extraction

T2W MRI images of patients were uploaded to the 3D slicer program in DICOM format (version 4.10.2; https://www.slicer.org). Resampled images (size:1x1x1 mm) were acquired and normalized to obtain isotropic voxels. The ovaries were segmented independently by two radiologists with 8 and 10 years of experience in abdominal radiology imaging. In all axial sections with ovaries, volume of interests (VOI) were obtained by manually segmenting the ovaries.

Eighteen first-order, 14 shape features, 75 texture features (gray-level co- occurrence matrix (GLCM), gray-level dependence matrix (GLDM), gray-level run length matrix (GLRLM), gray-level size zone matrix (GLSZM), and neighborhood gray tone difference matrix (NGTDM)) and 744 wavelet-based texture features extracted from VOI's (Figure 1). A total of 851 features were extracted using Slicer-Radiomics (PyRadiomics v3.0.1). Twenty patients were randomly selected and their ovaries (n=40) were segmented independently by two radiologists. Interobserver agreement was evaluated for the inferred radiomic features.

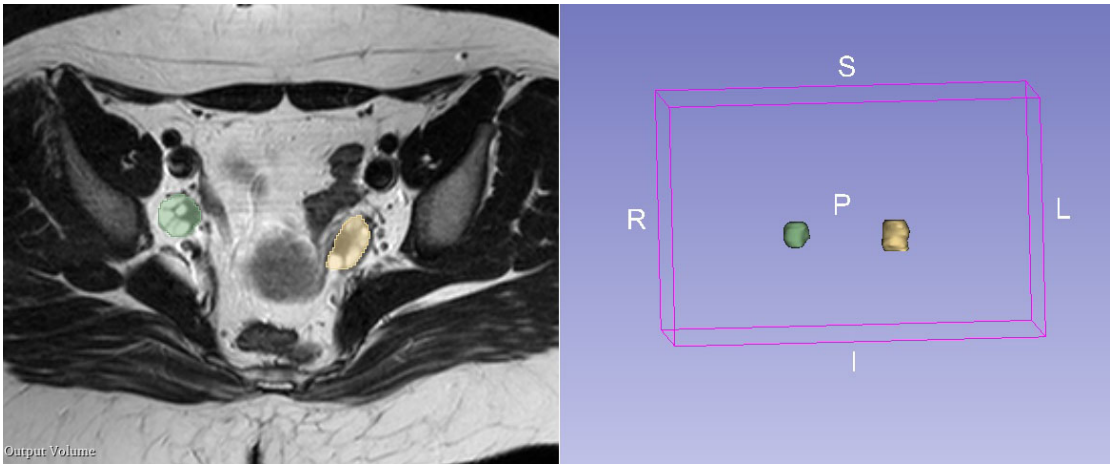

Figure 1. Manual segmentation of the ovary on axial T2-weighted images

Feature selection and model analysis

Python 2.3 (Jupyter Notebook, Pycaret Library) was used for data processing and machine learning (ML) analysis. ML analysis was performed on large numerical data sets of radiomic features. Binary classification was used to evaluate the predictive performance of radiomic features between two independent groups.

Feature reduction was performed for the features with the highest predictive performance. Potential predictive radiomic features were determined by univariate logistic regression analysis. Features with $p< 0.005$ in univariate regression analysis were re-analyzed using the least absolute shrinkage and selection operator (LASSO) regression method. Ten-fold cross validation was used to select features in the LASSO model with minimal criteria. Random Forest, Lasso regression and correlation-based feature selection were employed, with 0.75 as the threshold value for feature selection.

Datasets were randomly divided into train (70%) and

independent test (30%) datasets. A 10-fold cross-validation of the trained models was used to avoid data overfitting.

The prediction performances of the ML algorithm were evaluated using the mean area under the curve (AUC), accuracy, recall, precision, and F1 scores. The two best models for accuracy and AUC were determined and evaluated on the test set. A Receiver Operating Characteristic (ROC) curve was drawn. AUC, accuracy, recall, precision, and F1 scores were obtained from the confusion matrix. Cumulative distribution function (CDF) values of the groups were calculated with Kolmogrov Smirnov (KS) statistics. The distance between the CDFs of the two groups was given by the KS statistical graph. The blend model was tuned and finalized.

Statistical analysis

The study data were analyzed using the Statistical Package for Social Sciences (SPSS) version 25.0.0.0 software (IBM Corp., Armonk, N.Y., USA). Percentages, means, and standard deviations were used to summarize descriptive results. The one-sample Kolmogorov–Smirnov test was performed to check whether the groups followed a normal distribution. Continuous variables with a normal distribution were presented as mean (± standard deviation [SD]). ICC values were used to assess interobserver agreement. Categorical variables were compared with the chi-square test. Mann-Whitney U test was used to compare numerical data between two independent groups. Student's t-test was used to compare two independent groups for normally distributed numerical data. P-value <0.05 was considered statistically significant.

RESULTS

Data from 468 patients diagnosed with PCOS were evaluated. 348 patients without MRI were excluded from the study. MRIs of 120 patients who underwent pelvic MRI in our hospital were evaluated. 19 patients with artifacts were excluded from the study. The remaining 202 ovaries from 101 PCOS patients with an average age of 23±4 years were included in the study. Of the patients, 53 (52.5%) were phenotype A, 12 (11.9%) were phenotype B, 25 were phenotype C (25.1%), and 11 were phenotype D (10.9%). 130 (64.4%) of the ovaries were classical PCOS in group 0, 72 (35.6%) were non-classical PCOS in group 1. The characteristics of classical and nonclassical PCOS patients are presented in Table 1.

Table 1. Characteristics of classical and nonclassical PCOS patients

Parameters	Classic PCOS (n=65)	Non-classic PCOS (n=36)	P Value
Age (mean±SD)	23.18±4.42	22.36±4.13	P=0.28
BMI (mean±SD)	28.17±6.82	26.29±5.82	P=0.15
Oligo-amenorrhea (n,%)	64 (98.46 %)	11 (30.55 %)	P < 0.001
Hyperandrogenism (n, %)	46 (70.76 %)	34 (94.44 %)	P < 0.001
FG score (median, Q1-Q2)	10 (7,16)	8 (4,16)	P =0.03
Testosterone (median, Q1-Q2, ng/dl)	64 (42,88)	53.50 (42,79)	P =0.01
DHEAS level (mean±SD, ng/dl)	401.55±18	334.04±13	P=0.07
LH/FSH ratio(median, Q1-Q2)	1.07(0.60-2.28)	0.83 (0.52-1.72)	P=0.02
PCOM (n, %)	52 (80.00 %)	34 (94.44 %)	P = 0.001

Polycystic ovary syndrome, PCOS; BMI, body mass index; Ferriman-Gallwey (FG) score; dehidroepiandrosteron sulfat, DHEAS; luteinising hormone, LH; follicle stimulating hormone, FSH; Polycystic ovary morphology, PCOM.

A total of 851 features were extracted. 15 ML algorithms were used. The features selected by the ML algorithms are presented in Figure 2. Good interobserver reproducibility was obtained for these selected features (ICC 0.73-0.87). 141 ovaries were randomly divided into the training set and 61 ovaries into the test set.Accuracy and AUC in the training set were in the range of 57%-73% and 0.50-0.73, respectively (Table 2). Among the ML algorithms, the best two models were Random Forest (rf) (AUC:0.73, accuracy:73 %) and Gradient Boosting Classifier (gbc) (AUC:0.71, accuracy:70 %). AUC and accuracy

values in the test set were 0.73, 73% for Random Forest Classifier; for Gradient Boosting Classifier it was 0.70, 71% respectively. These two models were blended, and a new model was obtained. The blend model was tuned and finalized. The blend model's AUC, accuracy, recall and precision values and F1 score were 0.70, 73 %, 56 %, 66%, 58%, respectively. The confusion matrix and the classification report demonstrating the predictive performance of the blend model are given in Figure 3. ROC curve of blend model is presented in Figure 4. In the KS statistical plot, the distance between CDFs of the two groups had an average performance of 1 at a threshold of 0.17 (Figure 4).

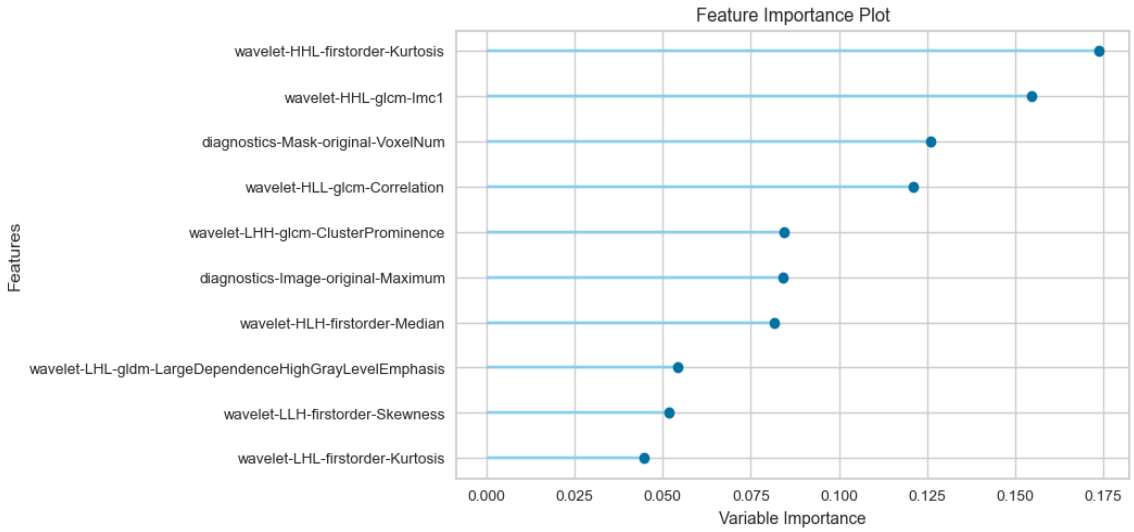

Figure 2. The features selected by the ML algorithms.

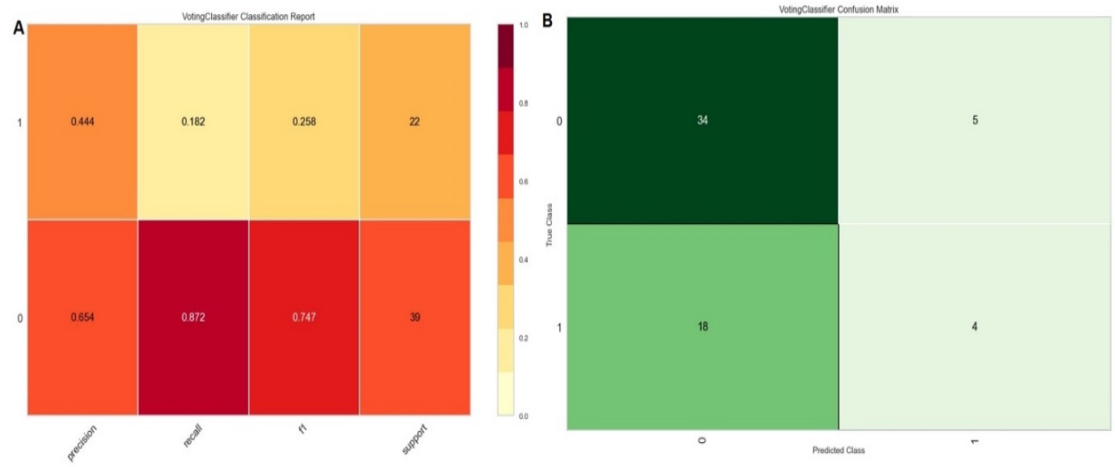

Figure 3. Classifier report and confusion matrix for blend model (Random Forest and Gradient Boosting Classifier) in distinguishing classical and non-classical PCOS.

Table 2. Performance of fifteen machine learning models in distinguishing classical and non-classical PCOS on the training set from T2-weighted sequences

Model	Accuracy	AUC	Recall	Precision	F1
Random Forest Classifier	0.7371	0.7382	0.4800	0.7038	0.5431
Light Gradient Boosting Machine	0.7290	0.7260	0.4800	0.7095	0.5430
Gradient Boosting Classifier	0.7162	0.7036	0.5200	0.6383	0.5651
Naive Bayes	0.6943	0.6547	0.4200	0.6150	0.4878
K Neighbors Classifier	0.6800	0.5796	0.5000	0.6245	0.5252
Extra Trees Classifier	0.6800	0.6946	0.3400	0.6595	0.4222
Logistic Regression	0.6519	0.6236	0.3000	0.5244	0.3419
Dummy Classifier	0.6452	0.5000	0.0000	0.0000	0.0000
Ridge Classifier	0.6448	0.0000	0.3000	0.4967	0.3392
Linear Discriminant Analysis	0.6448	0.6278	0.3000	0.4967	0.3392
Ada Boost Classifier	0.6110	0.6078	0.4000	0.4683	0.4190
Quadratic Discriminant Analysis	0.6090	0.5416	0.3200	0.3683	0.3350
Decision Tree Classifier	0.5948	0.5550	0.4200	0.4176	0.4020
SVM Linear Kernel	0.5762	0.0000	0.4200	0.4351	0.3865

Area under curve, AUC.

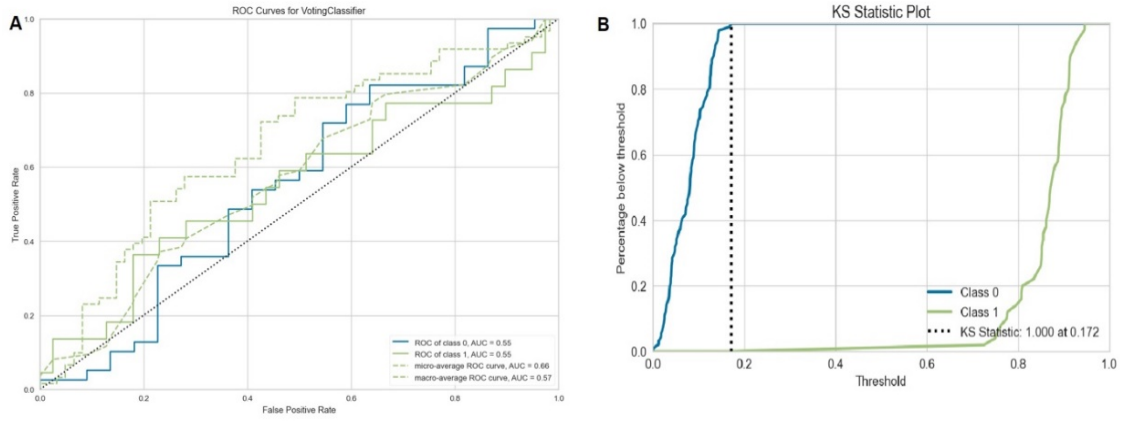

Figure 4. Receiver operating characteristics curve and Kolmogrov Smirnov statistical plot for blend model (Random Forest and Gradient Boosting Classifier) in distinguishing classical and non-classical PCOS.

DISCUSSION

Phenotypes of PCOS present with different clinical and metabolic findings, and treatment management varies accordingly. Phenotype is crucial in determining the treatment method and preventing complications. Phenotype A, which exhibits all the criteria of PCOS, is the most common type, while phenotype D, the mildest form, is the least common type[20,21]. Hyperandrogenism, insulin resistance, impaired lipid profile, and metabolic syndrome are more prevalent in phenotypes A and B, known as classical PCOS. Patients with these phenotypes are at higher risk for metabolic and cardiovascular diseases. Metabolic syndrome and insulin resistance are less common in phenotypes C and D, referred to as non-classical PCOS[3].

In a prior study by Razek et al., it was suggested that US findings, including ovarian volume, follicle number, follicle diameter and endometrial thickness, could distinguish classical PCOS from non-classical PCOS. The AUC values

of these findings were 0.79, 0.82, 0.83, and 0.77, respectively. The accuracy values were 75%, 73.6%, 79.2% and 68.1%, respectively. Sensitivity values

were between 71.7%-80.4% and specificity values were between 61.5-80.8%. Ovarian volume, the number of follicles, and follicle diameter were higher in classical PCOS than in non-classical PCOS[22]. In our study, we successfully differentiated classical PCOS from non-classical PCOS using radiomic features obtained from T2 sequences, achieving an AUC of 0.70 and an accuracy of 73%.

Primarily, first-order features were selected from the radiomics features in our study. The selection of first-order features, providing information about the signal intensity of the selected area, may be related to the number and peripheral distribution of follicles that are hyperintense in T2W. The voxel-number feature, which is an indicator of volume, was also highly correlated with classical PCOS.

Our study reported the most common phenotype A and the least phenotype D consistent with previous studies[23]. Varying rates are reported for phenotypes C and B. In our study, as observed in some previous studies, phenotype C was the second, and phenotype B was the third[24].

PCOS's heterogeneous nature with different phenotypes has been attributed to various hypotheses, such as interaction between genetic and environmental factors affecting PCOS pathogenesis or exposure to maternal androgens causing a specific phenotype in intrauterine life[25]. According to our study resluts, ovarian morphology and internal structure also vary according to phenotypes, suggesting that factors influencing PCOS development may contribute to different morphological effects in the ovary structure.

T2W-based radiomic features, according to our study results, are useful in distinguishing classical PCOS from non-classical PCOS, eve with a small number of patients, yielding acceptable AUC and accuracy values. Future studies with larger patient numbers could further support and enhance the AUC, accuracy, recall, and precision values.

Our study also revealed differences in ovarian morphology on MRI differs between classical and nonclassical PCOS. Radiomic features on MRI can objectively guide clinicians in distinguishing PCOS subgroups. Future studies, with larger patient groups, comparing the four phenotypes separately will provide more guidance on evaluating the effects on the ovarian parenchyma based on phenotypes.

The study's limitations include its retrospective nature and the small number of patients. Additionally, the study categorized patients into classical PCOS and nonclassical PCOS based on clinical and radiological findings, not considering the appearance of PCOM on US. Future studies should address these limitations.

In conclusion, MRI-based radiomic features may contribute to clinical evaluation in determining PCOS phenotypes. Early diagnosis is crucial for implementing effective treatment strategies and identifying high risk patients for metabolic and cardiovascular diseases, ultimately contributing to the preventing of potential comorbidities.

Author Contributions: Concept/Design : GR, SÖ, KA, MA, NF, AS; Data acquisition: GR, SÖ, KA; Data analysis and interpretation: GR, NF, AS, MA, HD, SE; Drafting manuscript: -; Critical revision of manuscript: GR, NF, ŞE, KA; Final approval and accountability: GR, NF, ATS, MA, HGD, ŞE, SÖ, KA, Technical or material support: GR, AS, NF, MA; Supervision: GR, KA, AS, NF, HGD; Securing funding (if available): n/a.
Ethical Approval: Kartal Dr, Lütfi Kırdar Şehir Hospital Ethical approval was obtained from the Clinical Research Ethics Committee with the decision dated 29.05.2023 and numbered 2023/514/250/35.
Peer-review: Externally peer-reviewed.
Conflict of Interest: Authors declared no conflict of interest.
Financial Disclosure: Authors declared no financial support

REFERENCES

1. Dumesic DA, Oberfield SE, Stener-Victorin E, Marshall JC, Laven JS, Legro RS. Scientific statement on the diagnostic criteria, epidemiology, pathophysiology, and molecular genetics of polycystic ovary syndrome. Endocr Rev. 2015;36:487-25.
2. Azziz R. Polycystic Ovary Syndrome. Obstet Gynecol. 2018;132:321-36.
3. Lizneva D, Suturina L, Walker W, Brakta S, Gavrilova-Jordan L, Azziz R. Criteria, prevalence, and phenotypes of polycystic ovary syndrome. Fertil Steril. 2016;106:6-15.
4. Rotterdam ESHRE/ASRM-Sponsored PCOS Consensus Workshop Group. Revised 2003 consensus on diagnostic criteria and long-term health risks related to polycystic ovary syndrome. Fertility and sterility. 2004;81:19-25.
5. Goodman NF, Cobin RH, Futterweit W, Glueck JS, Legro RS, Carmina E; American Association of Clinical Endocrinologists (AACE); American College of Endocrinology (ACE); Androgen Excess and PCOS Society (AES). American Association of Clinical Endocrinologists, American College of Endocrinology, And Androgen Excess And Pcos Society Disease State clinical review: guide to the best practices in the evaluation and treatment of polycystic ovary syndrome--part 1. Endocr Pract. 2015;21:1291-300.

6. Dewailly D, Lujan ME, Carmina E, Cedars MI, Laven J, Norman RJ et al. Definition and significance of polycystic ovarian morphology: a task force report from the Androgen Excess and Polycystic Ovary Syndrome Society. Hum Reprod Update. 2014;20:334-52.
7. Balen AH, Laven JS, Tan SL, Dewailly D. Ultrasound assessment of the polycystic ovary: international consensus definitions. Hum Reprod Update. 2003;9:505-14.
8. Rotterdam ESHRE/ASRM-Sponsored PCOS Consensus Workshop Group. Revised 2003 consensus on diagnostic criteria and long-term health risks related to polycystic ovary syndrome. Fertil Steril. 2004;81:19-25.
9. Brown M, Park AS, Shayya RF, Wolfson T, Su HI, Chang RJ. Ovarian imaging by magnetic resonance in adolescent girls with polycystic ovary syndrome and age-matched controls. J Magn Reson Imaging. 2013;38:689-93.
10. Kenigsberg LE, Agarwal C, Sin S, Shifteh K, Isasi CR, Crespi R, Ivanova J et al. Clinical utility of magnetic resonance imaging and ultrasonography for diagnosis of polycystic ovary syndrome in adolescent girls. Fertil Steril. 2015;104:1302-9.e94.
11. Kayemba-Kay's S, Pambou A, Heron A, Benosman SM. Polycystic ovary syndrome: Pelvic MRI as alternative to pelvic ultrasound for the diagnosis in overweight and obese adolescent girls. Int J Pediatr Adolesc Med. 2017;4:147-152.
12. Yoo RY, Sirlin CB, Gottschalk M, Chang RJ. Ovarian imaging by magnetic resonance in obese adolescent girls with polycystic ovary syndrome: a pilot study. Fertil Steril. 2005;84:985-95.
13. Fondin M, Rachas A, Huynh V, Franchi-Abella S, Teglas JP, Duranteau L et al. Polycystic Ovary syndrome in adolescents: which MR imaging-based diagnostic criteria?. Radiology. 2017;285:961-70.
14. Pereira-Eshraghi CF, Tao R, Chiuzan CC, Zhang Y, Shen W, Lerner JP et al. Ovarian follicle count by magnetic resonance imaging is greater in adolescents and young adults with polycystic ovary syndrome than in controls. F S Rep. 2022;3:102-9.
15. Aiyappan SK, Karpagam B, Vadanika V, Chidambaram PK, Vinayagam S, Saravanan KC. Age-related normogram for ovarian antral follicle count in women with polycystic ovary syndrome and comparison with age matched controls using magnetic resonance imaging. J Clin Diagn Res. 2016;10:11-3.
16. Lambin P, Leijenaar RTH, Deist TM, Peerlings J, de Jong EEC, van Timmeren J et al. Radiomics: the bridge between medical imaging and personalized medicine. Nat Rev Clin Oncol. 2017;14:749-62.
17. Rogers W, Thulasi Seetha S, Refaee TAG, Lieverse RIY, Granzier RWY, Ibrahim A, Keek SA, Sanduleanu S, Primakov SP, Beuque MPL, Marcus D, van der Wiel AMA, Zerka F, Oberije CJG, van Timmeren JE, Woodruff HC, Lambin P. Radiomics: from qualitative to quantitative imaging. Br J Radiol. 2020;93:2019-948.
18. Yildiz, B.O., Bozdag, G., Harmanci, A. Otegen U, Boynukalin K, Vural Z et al. Increased circulating soluble P-selectin in polycystic ovary syndrome. Fertility and Sterility. 201;93:2311–15.
19. Yildiz, B.O., Bolour, S., Woods, K. et al.Visually scoring hirsutism. Hum Reprod Update. 2010;16:51–64.
20. Mumusoglu, S., Yildiz, B. O. Polycystic ovary syndrome phenotypes and prevalence: differential impact of diagnostic criteria and clinical versus unselected population. Current Opinion in Endocrine and Metabolic Research. 2020;12:66-71.
21. Sachdeva G, Gainder S, Suri V, Sachdeva N, Chopra S. Comparison of the different PCOS phenotypes based on clinical metabolic, and hormonal profile, and their response to clomiphene. Indian J Endocrinol Metab. 2019;23:326-31.
22. Razek AAKA, Elatta HA. Differentiation Between Phenotypes of Polycystic Ovarian Syndrome With Sonography. Journal of Diagnostic Medical Sonography. 2021;37:337-44.
23. Lizneva D, Kirubakaran R, Mykhalchenko K, Suturina L, Chernukha G, Diamond MP et al. Phenotypes and body mass in women with polycystic ovary syndrome identified in referral versus unselected populations: systematic review and meta-analysis. Fertil Steril. 2016;106:1510-20.
24. Carmina E, Campagna AM, Lobo RA. A 20-year follow-up of young women with polycystic ovary syndrome. Obstet Gynecol. 2012;119:263-9.
25. Ladrón de Guevara A, Fux-Otta C, Crisosto N, Szafryk de Mereshian P, Echiburú B, Iraci G et al. Metabolic profile of the different phenotypes of polycystic ovary syndrome in two Latin American populations. Fertil Steril. 2014;101:1732-9.
26. Franks S, McCarthy MI, Hardy K. Development of polycystic ovary syndrome: involvement of genetic and environmental factors. Int J Androl. 2006;29:278-90.